



HAL
open science

INFLUENCE OF THE WOLLASTONITE AND GLASS FIBERS ON GEOPOLYMER COMPOSITES WORKABILITY AND MECHANICAL PROPERTIES

Julien Archez, Nathalie Texier-Mandoki, Xavier Bourbon, Jean-François Caron, S. Rossignol

► **To cite this version:**

Julien Archez, Nathalie Texier-Mandoki, Xavier Bourbon, Jean-François Caron, S. Rossignol. INFLUENCE OF THE WOLLASTONITE AND GLASS FIBERS ON GEOPOLYMER COMPOSITES WORKABILITY AND MECHANICAL PROPERTIES. *Construction and Building Materials*, 2020, 257, pp.119511. 10.1016/j.conbuildmat.2020.119511 . hal-02934613

HAL Id: hal-02934613

<https://enpc.hal.science/hal-02934613v1>

Submitted on 9 Sep 2020

HAL is a multi-disciplinary open access archive for the deposit and dissemination of scientific research documents, whether they are published or not. The documents may come from teaching and research institutions in France or abroad, or from public or private research centers.

L'archive ouverte pluridisciplinaire **HAL**, est destinée au dépôt et à la diffusion de documents scientifiques de niveau recherche, publiés ou non, émanant des établissements d'enseignement et de recherche français ou étrangers, des laboratoires publics ou privés.

INFLUENCE OF THE WOLLASTONITE AND GLASS FIBERS ON GEOPOLYMER COMPOSITES WORKABILITY AND MECHANICAL PROPERTIES

J. Archez^{1,2,3}, N. Texier-Mandoki², X. Bourbon², J.F. Caron³ and S. Rossignol¹

¹ IRCER: Institut de Recherche sur les Céramiques (UMR7315), 12 rue Atlantis, 87068 Limoges Cedex, France.

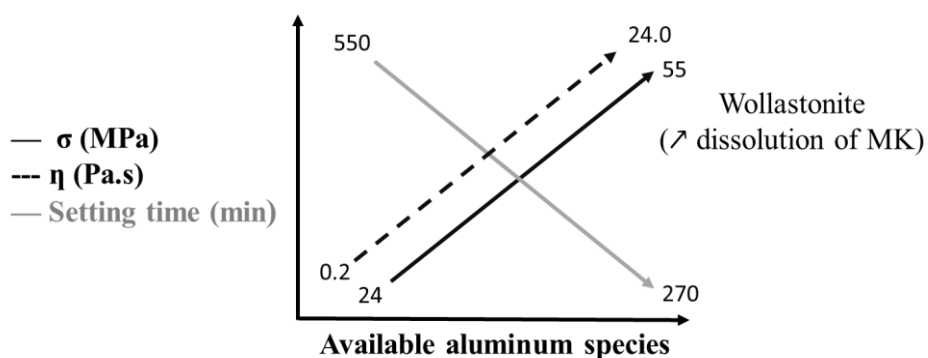
² Agence nationale pour la gestion des déchets radioactifs (Andra), 1/7 rue Jean-Monnet 92298 Chatenay-Malabry Cedex, France.

³ Laboratoire Navier, UMR 8205, Ecole des Ponts, CNRS, UPE, Champs-sur-Marne, France

■ Corresponding author: sylvie.rossignol@unilim.fr, tel.: 33 5 87 50 25 64

Aluminum concentration	Fiber	Composite
Viscosity	Wollastonite	Geopolymer

Graphical abstract



Highlights

- Geopolymer composites based on wollastonite and glass fibers were synthesized
- Influence of the MK and additives on viscosity and working properties was studied
- The wollastonite ensures a better dissolution of the metakaolin
- The glass fibers act as an anchoring site during the geopolymerization reaction
- The aluminum concentration enables to monitor the viscosity and compressive strength

Abstract

This work aims to synthesize geopolymer composites and study the influence of the aluminum concentration, wollastonite and glass fibers on the properties of the fresh and hardened material. To this end, different metakaolin, wollastonite and glass fibers contents were used to synthesize geopolymer composites. The effect of reinforcement elements on the geopolymerization reaction has then been studied with FTIR spectroscopy and thermal analysis (DTA-TGA). Moreover, the viscosity and the setting time of the reactive mixture, as well as the compressive strength of the hardened material, have been measured for the different compositions. The results showed that the nature of the reinforcement added induces different polycondensation reactions. The wollastonite improves the viscosity and the mechanical properties by ensuring a better dissolution of the metakaolin, whereas the glass fibers act as an anchoring site during the geopolymerization reaction, leading to a ductile failure of the material. Finally, the aluminum concentration enables to monitor the viscosity and setting time of the reactive mixture and has a significant influence on the microstructure and the compressive strength. Thus, the initial formulation of the geopolymer composites allows controlling the properties of the fresh and hardened geopolymer composites.

I. INTRODUCTION

The French National Radioactive Waste Management Agency (Andra) has plans for a long-term management of the high- and intermediate-level radioactive wastes in a deep geological disposal. This project, named Cigéo (industrial waste disposal facility) has been studied for decades and will be built in the eastern Parisian Basin (France). The design concept for this high-level disposal consists of a seventy-centimeter steel liner in which waste packages will be placed. However, this steel liner can present corrosion. An alternative material such as previously studied alkali-activated materials [1] is therefore investigated to prevent corrosion. For this application, the material properties prevail on its price. The material has to be inorganic, be resilient to radial flexion and anisotropic mechanical stress and required mechanical stability for, at least, as long as the operating period. Thus, the geopolymers' structures have to be examined in order to satisfy the specifications required.

Geopolymers are mineral amorphous three-dimensional aluminosilicate materials, synthesized by the activation of an aluminosilicate source by an alkaline solution at ambient temperature and present acid and fire resistance [2, 3]. FTIR spectroscopy has previously been used to study the synthesis of gels and geopolymer materials, in order to analyze the geopolymerization reaction over time [4]. The following of the spectra over time permit to follow the evolution of the various contributions relating to the intense bond of the Q² species (Si-O-Si). During this reaction, the substitution of the silicon by the aluminum atoms issue from the metakaolin favors the formation of Si-O-Al bonds, as the FTIR band at 984 cm⁻¹ (Q² type Si-O-M, M=Si or Al) shifts to a lower value [5]. Besides, it has been shown that a shift value close to 22 cm⁻¹ is characteristic of the formation of a geopolymer network, whereas higher values outline the formation of several networks. Moreover, the concentration of aluminum (AlOH₄⁻ species) is an important parameter in the geopolymer formation, as it is involved in the geopolymerization reaction. Indeed, an increase in the aluminosilicate source content, such as

fly ash [6] or metakaolin [7], leads to an increase in reactive aluminum rate in the reactive mixture and the viscosity increases. Similarly, the decrease in alkali and aluminum concentrations delays the geopolymer's solidification [8]. Furthermore, the quantity of reactive aluminum in the raw materials allows having an influence on the mechanical properties of the geopolymer binder [9]. Autef *et al.* [10] studied various metakaolins and have shown that their reactivity can lead to different network structures, and thus to different mechanical properties. Gharzouni *et al.* [11] studied different formulations for different alkaline solution-metakaolin mixtures, and concluded that the high reactivity of the precursors induces a higher densification degree through the apparition of small colloids. Jaya *et al.* [12] suggested that a balanced metakaolin to alkali activator *ratio* shall ensure the optimum dissolution of the metakaolin and the limitation of unreacted particles. All in all, it is possible to decrease the solid to liquid *ratio* (S/L), thus slowing down the polycondensation reaction, and resulting in the creation of several networks, as well as the withholding of a higher amount of water in the geopolymer [5, 13]. On the contrary, increasing the reactive aluminosilicate source promotes the polycondensation reaction and thus lowers the water content retained in the samples. This water content can be determined with differential thermal analysis (DTA) and thermogravimetric analysis (TGA), where the weight loss measured is specific to the quantity of physisorbed, poral and structural water in the geopolymer, which can then be related to the geopolymer network and may have an influence on its mechanical properties [14]. The workability (viscosity, setting time) of the geopolymer can be determined by following the viscosity value as a function of time with a viscometer apparatus [8]. Viscosity values of the reactive mixture depend on the viscosity of the alkaline solution [15], the fraction volume [16] but also the water content and the alkaline concentration of the reactive mixture [7]. Viscosity and setting can also be modified with the use of additives such as orthophosphoric acid or decahydrated borax [17]. The workability and the mechanical properties of geopolymers binders are already well studied and achieved in the

literature [18, 19]. However, geopolymer binders present a brittle behavior. Reinforcement elements are therefore needed to be added to form a composite based on a geopolymer matrix, to enhance the mechanical strength to validate the specifications.

Reinforcement fibers have first been used in 1982 by J. Davidovits [20], to develop molding tools for the plastic industry, enabling an increase in tensile and flexural strength, thus preventing brittle failure by monitoring the crack opening and its diffusion throughout the material [21]. Similarly, Li *et al.* [22] used polyvinyl alcohol short fibers to elaborate a reinforced geopolymer, improving the flexural strength and the ductility of the material. Moreover, introducing those reinforcement elements modifies the granular skeleton of the material. Santos *et al.* [23] have indeed demonstrated that a continuous granular skeleton leads to a better compressive strength in the case of self-compacting concrete. Short fibers (length < 20 mm) are the most commonly used reinforcement elements for castable materials, as they can be easily mixed and casted within the geopolymer matrix. Different types of short inorganic fibers, such as carbon fibers [24], silicon carbide fibers [25], basalt fibers [26, 27] or glass fibers [28, 29], have been successfully utilized with metakaolin-based geopolymers. Moreover, glass fibers have been used with alkali-activated composites based on fly ash [30, 31] to improve the flexural modulus, thus modifying the post-cracking response by enhancing the ductility of the material after the first crack. Needles of wollastonite have been used as well, in order to enhance the mechanical performance of hydrated cements [32], alkali-activated mortars [33] or composites [34]. According to a review on fiber-reinforced metakaolin-based geopolymer composites [18], the compressive and flexural strength values range from 14 to 109 MPa and from 3 to 14 MPa respectively, depending on the matrix and the nature and quantity of the fibers used. Moreover, the addition of fibers into the matrix improves the viscosity of the mixture prior to setting, depending on the quantity, type and aspect *ratio* of the fibers [35]. The use of mineral reinforcement elements could therefore increase the mechanical properties of the

geopolymer binder. However, the addition of wollastonite [36] or glass fibers [30] increases the viscosity and decreases the workability.

Few studies have been carried out in order to evaluate the influence of the wollastonite and glass fibers on the availability of aluminum on the geopolymerization reaction. Thus, the aim of this work was to assess the impact of the formulation (metakaolin and reinforcement elements) on the workability and on the mechanical properties of the geopolymer composites.

II. Experimental

1. Raw materials and samples preparation

Two mineral reinforcement elements with different dimensions and compositions (glass fibers and wollastonite) have been used to reinforce the metakaolin-based geopolymer binders previously studied [37]. Glass fibers are alkaline resistant (L. = 6 mm, D. = 13-15 μm) and wollastonite are acicular particles (L. = 5-170 μm , D. = 3-15 μm). The different raw materials used to prepare the geopolymer binders and composites are gathered in **Table 1**. A fixed quantity of a commercial solution, with a silicon to potassium (Si/K) molar *ratio* of 1.70 reduced to 0.58 by dissolving pellets of KOH *via* magnetic stirring during five minutes, has been mixed with different quantities of a commercial metakaolin (Si/Al = 1.17) (**Table 1**). A commercial metakaolin (M1000) provided by Imerys was added in different ratios.

The experimental process to prepare the geopolymer samples is described in **Figure 1**. The geopolymer binders were synthesized by adding the metakaolin in the silicate alkaline solution, then mixing it with a stirring blade to obtain 60 cm^3 of reactive mixture. Three geopolymer binders, already studied in the IRCER laboratory [38], were used in this work. They present different amount of metakaolin in a fixed volume of solution (solid to liquid ratio equals to 0.6, 0.8 and 1.0). Different amount of glass fibers and/or wollastonite (**Table 1**) were then added to this geopolymer binders to obtain a geopolymer composite and to study the influence of these reinforcement elements on geopolymer binders. The resulting mixture was

mixed until obtaining a homogenous mixture during a total time of ten minutes and was then casted in a closed sealable polystyrene mold at room temperature (20°C).

The nomenclature used is aM_xW_yG_z , where M, W and G stand for the Metakaolin, the Wollastonite and the Glass fibers respectively, whereas a refers to the metakaolin to alkaline solution mass *ratio* (a being 0.6, 0.8 or 1.0), with $a = 0.6$ and $a = 1$ defining respectively a low metakaolin amount (low aluminum concentration) and a high metakaolin amount (high aluminum concentration). Finally, x , y and z represent the weight percentage of metakaolin, wollastonite and glass fibers respectively, with their sum being 100. The compositions, codes and nomenclatures of the different aM_xW_yG_z samples are presented in **Table 2**. As an example, for 19 g of solution, 12 g of metakaolin, 2.70 g of wollastonite and 0.68 g of glass fibers, a will be equal to 0.6 and the composite will be referenced as ${}^{0.6}M_{78}W_{18}G_4$.

2. Sample characterization

The viscosity measurements were carried out on a Brookfield DV-II viscometer (with an estimated error of 1 %) on 60 cm³ of reactive mixture in a cylindrical container, every 30 minutes, in agreement with the setting time, while maintaining the stirring on a lab roller at 60 rpm in an air conditioned room at 20 °C. The average viscosity value was determined over a one-minute measurement, and the spindle's speed was set according to the viscosity, with values ranging from 0.1 to 100 rpm. The maximum viscosity value measurable was 6000 Pa.s, which would be the case for an almost consolidated material. The initial viscosity of the reactive mixture was determined twenty minutes after mixing the raw materials, and the setting time was calculated with the tangent method applied to the curve showing the viscosity as a function of time [7].

Fourier-transform infrared (FTIR) spectra were collected with the Attenuated Total Reflectance (ATR) mode, with a 4 cm⁻¹ resolution over a range from 400 to 4000 cm⁻¹. The contribution of the atmospheric CO₂ was removed *via* a straight-line fit between 2400 and 2280

cm⁻¹. The spectra were then baseline corrected and normalized to ease further comparisons. Besides, in order to monitor the geopolymer's formation, a software was used to acquire a 64-scans spectrum every 10 min during 12 hours.

Differential Thermal Analysis (DTA) and Thermogravimetric Analysis (TGA) were carried out in platinum crucibles on an SDT Q600 apparatus from TA Instruments, using Pt/Pt - 10 % Rh thermocouples under a flowing dry-air atmosphere (100 cm³/min). The powder samples were stored at 20°C and 80 % relative humidity, and then heated up to 1000 °C with a 5 °C.min⁻¹ heating slope.

The normal compressive strengths were evaluated using an Instron 5969 with a 50 kN load cell at a constant speed of 0.5 mm.min⁻¹, and were measured for every compositions after seven days on ten cylindrical samples, with a 15 mm diameter and a 30 mm height. The final compressive strength values represent an average over ten measurements.

The morphology of the final material was analyzed using a JEOL IT 300 LV scanning electron microscope at 10 kV. The fractured samples were kept after their compressive strength tests, set on carbon paste and then sprayed with a 10 nm layer of Pt before observations.

III. RESULTS

1) Effect of reinforcement elements on the polycondensation reaction

A geopolymer binder and three geopolymer composites based on wollastonite and/or glass fibers (^{0.6}M₁₀₀, ^{0.6}M₇₀W₃₀, ^{0.6}M₉₀G₁₀ and ^{0.6}M₇₈W₁₈G₄) were selected to analyse the influence of the mineral reinforcement elements on the geopolymer network. To this end, FTIR analyses and thermal measurements were carried out on the reactive mixture to determine the water content, in order to understand the effect of reinforcement elements on the polycondensation reaction.

The FTIR spectra at $t = 0$ and $t = 700$ min relative to the compositions $^{0.6}\text{M}_{100}$, $^{0.6}\text{M}_{70}\text{W}_{30}$, $^{0.6}\text{M}_{90}\text{G}_{10}$ and $^{0.6}\text{M}_{78}\text{W}_{18}\text{G}_4$, are gathered in **Figure 2**. All the spectra present modifications over time for the Si-OH and $\nu\text{H}_2\text{O}$ contributions, as well as for the Si-O- M (with $M = \text{Si}, \text{Al}$) bond. At $t = 0$ min, the $^{0.6}\text{M}_{100}$ sample displays three contributions centered at 3400, 1600 and 984 cm^{-1} , that can be assigned to the νOH , δOH and $\nu\text{Si-O-}M$ bonds, respectively [4]. After 700 minutes, the same features are observed; however, the intensity of the water contributions decreases and the Si-O- M (with $M = \text{Si}, \text{Al}$) bond shifts to lower wavenumbers, due to the polycondensation reaction [5]. Concerning the $^{0.6}\text{M}_{100}$ geopolymer, the Si-O- M shift is equal to 45 cm^{-1} , whereas the $^{0.6}\text{M}_{70}\text{W}_{30}$, $^{0.6}\text{M}_{90}\text{G}_{10}$ and $^{0.6}\text{M}_{78}\text{W}_{18}\text{G}_4$ samples, though exhibiting the same behavior, have lower shift values of 33, 16 and 22 cm^{-1} , respectively. Those different variations underline the formation of Si-O-Al bonds, characteristic of the geopolymer network formation, and emphasize the influence of the aluminum concentration on this network.

The evolution of the Si-O- M bond's position as a function of time for the different compositions is displayed in **Figure 3**. The $^{0.6}\text{M}_{100}$ geopolymer reaches a shift of 45 cm^{-1} following a 0.16 $\text{cm}^{-1} \cdot \text{min}^{-1}$ slope, whereas, with the presence of wollastonite ($^{0.6}\text{M}_{70}\text{W}_{30}$), the shift presents a delay before reaching 33 cm^{-1} following a similar slope (0.15 $\text{cm}^{-1} \cdot \text{min}^{-1}$). These differences may be due to a change in the reactional mixture and a modification of the speciation equilibrium of species. Furthermore, the composite $^{0.6}\text{M}_{90}\text{G}_{10}$ displays a lower shift of 16 cm^{-1} with a 0.03 $\text{cm}^{-1} \cdot \text{min}^{-1}$ slope, due to the steric hindrance caused by the integration of the glass fibers [7]. This can be considered to be the result of two effects. On the one hand, the reaction between the species forming the network and the Si-O-Si sites from the glass fibers does not change the initial wavenumber value. In effect, the fibers may act as an anchoring site without any chemical reactivity [7]. On the other hand, the polycondensation reactions are inhibited by the Si-O-Si sites of the glass fibers, inducing the shift and modifying the geopolymer network. Finally, the mixture with both the wollastonite and the glass fibers ($^{0.6}\text{M}_{78}\text{W}_{18}\text{G}_4$) presents a

shift of 22 cm^{-1} and a $0.03 \text{ cm}^{-1} \cdot \text{min}^{-1}$ slope which are characteristic of the effects attributed to the reinforcement elements. Thus, the addition of wollastonite and glass fibers seem to respectively promote and initiate the polycondensation reactions.

Differential thermal and thermogravimetric analyses were carried out for the $^{0.6}\text{M}_{100}$, $^{0.6}\text{M}_{70}\text{W}_{30}$, $^{0.6}\text{M}_{90}\text{G}_{10}$ and $^{0.6}\text{M}_{78}\text{W}_{18}\text{G}_4$ samples between 25 and 1000 °C (Figure 4). All the samples present the same trend, with a major weight loss between 20 and 200 °C, which can be related to an endothermic peak typical of the loss of water described in the literature [5]. Above 900 °C, an exothermic peak can be assigned to the transformation of the amorphous silica structure into a aluminosilicate-type phase (spinel or mullite) [5]. The weight loss of the geopolymer without reinforcements (Figure 4a), can be attributed to the losses of physisorbed water between 25 and 42 °C, of poral water between 42 and 200 °C (I) and of structural water between 200 and 1000 °C (II) [5]. Thus, as for the $^{0.6}\text{M}_{100}$ sample, the poral and structural combined weight loss between 42 and 1000 °C (I + II) is equal to 29 %, whereas it is lower, 22 % in the same interval of temperature, with the addition of the wollastonite ($^{0.6}\text{M}_{70}\text{W}_{30}$) as shown on Figure 4b. However, it is to be noticed that, concerning this last sample, considering only geopolymer matrix with no interaction induced by wollastonite, the combined weight loss would be equal to 25%. Thus, the difference in weight losses (25 and 22 %) can underline the influence of the addition of wollastonite on the polycondensation reaction. Finally, the $^{0.6}\text{M}_{90}\text{G}_{10}$ composition with glass fibers presents the same weight loss as the $^{0.6}\text{M}_{100}$ geopolymer (28 and 29 % respectively as shown on Figure 4c), whereas the $^{0.6}\text{M}_{78}\text{W}_{18}\text{G}_4$ sample displays a weight loss of 24 %, which is an intermediate value standing between the composites containing wollastonite ($^{0.6}\text{M}_{70}\text{W}_{30}$) and glass fibers ($^{0.6}\text{M}_{90}\text{G}_{10}$) (Figure 4d).

2) Workability in function of metakaolin and reinforcement elements

In order to understand the effect of metakaolin and reinforcement elements on workability, Figure 5 presents the logarithmic evolution of the viscosity as a function of time

for the different formulations of the reactive mixture, *i.e.* $^{0.6}\text{M}_{100}$, $^{0.8}\text{M}_{100}$, and $^1\text{M}_{100}$ (**Figure 5a**), $^{0.6}\text{M}_{70}\text{W}_{30}$, $^{0.6}\text{M}_{45}\text{W}_{55}$, $^{0.6}\text{M}_{90}\text{G}_{10}$ (**Figure 5b**) and $^{0.6}\text{M}_{78}\text{W}_{18}\text{G}_4$, $^{0.8}\text{M}_{85}\text{W}_{11}\text{G}_4$ and $^1\text{M}_{87}\text{W}_{10}\text{G}_3$ (**Figure 5c**). All the geopolymer mixtures display the same tendency: their curves display a quasi-plateau followed by a steep raise up to the viscometer's measurement limit of 6000 Pa.s. The setting time has been determined as the point of intersection of the tangent lines to the two parts of the curve [8]. Thus, the initial viscosity and the setting time of the $^{0.6}\text{M}_{100}$ sample (**Figure 5a**), are equal to 0.17 Pa.s and 487 minutes respectively. Moreover, it appears that an increase in the metakaolin quantity in the initial mixture ($^{0.6}\text{M}_{100}$ to $^1\text{M}_{100}$), leads to an increase in the initial viscosity from 0.17 to 2.66 Pa.s and a decreased setting time from 487 down to 273 minutes. These two effects can be explained by the greater amount of reactive aluminum introduced through the metakaolin, thus promoting the polycondensation reactions. Similarly, the influence of wollastonite on the evolution of the $^{0.6}\text{M}_{100}$ reactive mixture can be deduced from **Figure 5b**, where an increase in the wollastonite content (from the mixture $^{0.6}\text{M}_{70}\text{W}_{30}$ to $^{0.6}\text{M}_{45}\text{W}_{55}$) leads to a higher initial viscosity raising from 1.28 to 21.8 Pa.s and to a lower setting time from 469 down to 396 minutes. This may be linked to the water demand of the wollastonite and the greater availability of the reactive species [7]. On the other hand, the addition of glass fibers ($^{0.6}\text{M}_{90}\text{G}_{10}$) has only a slight impact on the initial viscosity and the setting time, which may be linked to a low content and a homogenous dispersion of the glass fibers in the mixture [39]. Finally, the influence of the addition of both the wollastonite and the glass fibers mixed with different metakaolin amounts ($^{0.6}\text{M}_{78}\text{W}_{18}\text{G}_4$, $^{0.8}\text{M}_{85}\text{W}_{11}\text{G}_4$ and $^1\text{M}_{87}\text{W}_{10}\text{G}_3$) can be extracted from **Figure 5c**. As seen previously, both the additions of metakaolin ($^{0.8}\text{M}$ and ^1M) and of reinforcement elements increase the viscosity. Additionally, the composite $^1\text{M}_{87}\text{W}_{10}\text{G}_3$ has an initial viscosity three times higher than the $^1\text{M}_{100}$ sample, thanks to the effect of both reinforcement elements.

In the end, the viscosity of the reactive mixture is enhanced by the addition of both the metakaolin and the reinforcement elements, while the setting time is mainly controlled by the sole metakaolin amount introduced.

3) Microstructure and mechanical properties of the geopolymer composites

Compressive strength tests were carried out in order to evaluate the influence of the quantity of the metakaolin and/or the reinforcement elements on the mechanical properties of the hardened material. The compressive strength of the different composites as a function of the strain (measured with the displacement of the machine), is shown in **Figure 6**, varying quite significantly depending on the binder and the nature and quantity of the reinforcement elements. It appears that the geopolymer binders (**Figure 6a**) are characterized by a linear variation, typical of an elastic regime, followed by a non-linear deformation and a brittle failure, while a higher quantity of metakaolin introduced induces a higher compressive strength (55 and 32 MPa for $^1M_{100}$ and $^{0.6}M_{100}$, respectively). This result is in agreement with the work carried out by Gharzouni *et al.* [37], who have demonstrated that an increase in the reactive aluminum amount leads to an increase in the compressive strength of the geopolymer. The addition of wollastonite (**Figure 6b**) in the $^{0.6}M$ geopolymer leads to a higher compressive strength (from 32 ± 3 for $^{0.6}M_{100}$, to 47 ± 3 MPa for $^{0.6}M_{45}W_{55}$). The failure mode remains fragile for a small amount of wollastonite ($^{0.6}M_{70}W_{30}$) and becomes ductile with a higher amount ($^{0.6}M_{45}W_{55}$). This might be explained by the modification of the granular skeleton by the micrometric acicular wollastonite [23], and by the modification of the geopolymer network, as previously seen with FTIR spectroscopy and thermal measurements. The addition of glass fibers in the $^{0.6}M$ geopolymer ($^{0.6}M_{90}G_{10}$) leads to a decrease in both the compressive strength by 56% and in the slope of the elastic regime (Young modulus). This effect may be a consequence of the modification of the granular skeleton due to the steric hindrance of the glass fibers [35], transforming the brittle failure into a ductile failure [30]. Mixing wollastonite and glass fibers

within the $^{0.6}\text{M}$, $^{0.8}\text{M}$ and ^1M geopolymer binders leads to different behaviors, depending on the amount of metakaolin and reinforcement elements (**Figure 6c**), thus, the addition of wollastonite and glass fibers ($^{0.6}\text{M}_{78}\text{W}_{18}\text{G}_4$) exhibits a ductile failure typical of composites. A similar behavior is observed for the $^{0.8}\text{M}_{85}\text{W}_{11}\text{G}_4$ composition, whereas a higher metakaolin amount coupled with lower reinforcement elements amounts ($^1\text{M}_{87}\text{W}_{10}\text{G}_3$) results in a brittle failure. Therefore, the metakaolin amount has a significant influence on the maximum stress of the geopolymer composites, while the compressive strength and failure mode are mainly driven by the reinforcement elements, especially in the case of the low metakaolin content samples ($^{0.6}\text{M}$ and $^{0.8}\text{M}$).

The addition of both metakaolin and mineral reinforcements has a direct impact on the aluminum concentration, respectively raising it or reducing it slightly. The metakaolin brings silicon and reactive aluminum and increase the aluminum concentration. However, the reinforcement elements bring no reactive aluminum and the volume (calculated with the density) increases. That leads to a slight decrease of the aluminum concentration. Moreover, modifying this concentration enables to obtain diverse geopolymer formations differentiated by their viscosity or setting time, thus resulting in different mechanical properties. In order to have a more precise understanding of the effect of the amount of metakaolin and reinforcement elements introduced in the mixture, the initial viscosity, the density and the maximum compressive strength are presented in **Figure 7** as functions of the aluminum concentration for $^a\text{M}_x\text{W}_y\text{G}_z$ samples (**Table 2**).

With the addition of wollastonite forming the compounds $^{0.6}\text{M}_{45}\text{W}_{55}$ and $^1\text{M}_{78}\text{W}_{22}$, the initial viscosities of the $^{0.6}\text{M}_{100}$ (0.18 Pa.s) and $^1\text{M}_{100}$ (2.66 Pa.s) geopolymers increase to 21.9 and 23.8 Pa.s, respectively (**Figure 7a**). Similarly, the addition of glass fibers leading to the $^{0.6}\text{M}_{90}\text{G}_{10}$ and $^1\text{M}_{94}\text{G}_6$ samples increases the initial viscosity to 0.28 and 5.63 Pa.s from 0.18 and 2.66 Pa.s, respectively. Thus, the addition of wollastonite raises strongly the viscosity of the reactive

mixture, depending on the percentage of wollastonite added and regardless of the amount of metakaolin. The glass fibers appear to share the same effect, but have to be used in limited quantity because of the steric hindrance of the fiber. Three tendencies ($a = 0.6, 0.8$ or 1) are then observed for the initial viscosity, where the higher the aluminum concentration (directly linked to the amount of metakaolin introduced) in the initial blend is, the higher the viscosity is. Moreover, for an equal amount of metakaolin, the viscosity improves with the addition of reinforcement elements, while the concentration of aluminum drops slightly. Thus, glass fibers seem to increase the viscosity due to the steric hindrance, whereas the wollastonite induces an increase due to the water demand of the reinforcing element.

The density of the geopolymer binders $^{0.6}\text{M}_{100}$, $^{0.8}\text{M}_{100}$ and $^1\text{M}_{100}$, presented in **Figure 7b**, increases with the aluminum concentration, displaying values of $1.57, 1.64$ and 1.72 g.cm^{-3} for $7.3, 8.9$ and 10.3 mol.L^{-1} , respectively. Furthermore, both the additions of wollastonite ($^{0.6}\text{M}_{45}\text{W}_{55}$) and glass fibers ($^{0.6}\text{M}_{90}\text{G}_{10}$) increase the density to 1.86 g.cm^{-3} and 1.60 g.cm^{-3} respectively, regardless of the metakaolin content. Similarly, diminishing the aluminum concentration with the addition of wollastonite and fibers leads to an enhancement of the geopolymer composite's density by modifying its granular skeleton [23].

The compressive strength of the binders $^{0.6}\text{M}_{100}$, $^{0.8}\text{M}_{100}$ and $^1\text{M}_{100}$ raises with the aluminum concentration from 32 to 55 MPa , in agreement with the relation between the aluminum rate and the geopolymerization reaction (**Figure 7c**) [40]. The addition of wollastonite ($^{0.6}\text{M}_{70}\text{W}_{30}$) in low metakaolin compositions ($^{0.6}\text{M}$) increases the compressive strength up to 40 ± 3 from $32 \pm 3 \text{ MPa}$ respectively, whereas it appears to have no influence on compositions with high metakaolin (^1M), reaching respectively 55 ± 3 and $53 \pm 3 \text{ MPa}$ for the $^1\text{M}_{100}$ and $^1\text{M}_{70}\text{W}_{30}$ samples. Thus, the granular skeleton of a high metakaolin composition does not seem to be enhanced by the addition of wollastonite. Besides, the addition of glass fibers ($^a\text{M}_x\text{G}_y$ with $a = 0.6, 0.8$ or 1) leads to a slight decrease in the compressive strength ($32 \pm 3 \text{ MPa}$ down to $22 \pm$

3 MPa for ${}^1M_{100}$ and ${}^1M_{90}G_{10}$ respectively), due to the steric hindrance of the glass fibers [7]. The aluminum and compressive strength both decrease slightly with the additions of wollastonite and glass fibers (aM_xW_yG_z with $a = 0.6, 0.8$ or 1). Thus, the viscosity, the density and the mechanical properties are driven by the aluminum concentration, potentially modified by the quantities of metakaolin and reinforcement elements introduced

SEM micrographs are displayed in **Figure 8** for the ${}^{0.8}M_{100}$, ${}^{0.8}M_{74}W_{26}$, ${}^{0.8}M_{92}G_8$, ${}^{0.8}M_{85}W_{11}G_4$, ${}^{0.6}M_{70}W_{30}$, and ${}^1M_{78}W_{22}$ composites. The microstructure of the ${}^{0.8}M_{100}$ geopolymer binder observed in **Figure 8a** is typical of geopolymer materials [41]. Moreover, while the microstructure of the ${}^{0.8}M_{74}W_{26}$ sample (**Figure 8b**) is similar to the ${}^{0.8}M_{100}$ binder, suggesting that the wollastonite is dispersed throughout the geopolymer matrix, the microstructure of ${}^{0.8}M_{92}G_8$ seems different, due to the addition of glass fibers (**Figure 8c**), which seem to have low adhesion, resulting in small voids appearing between them and the geopolymer matrix. Finally, the ${}^{0.8}M_{85}W_{11}G_4$ sample, containing both reinforcement elements (**Figure 8d**), displays a similar microstructure with dispersed wollastonite and glass fibers within the matrix, whereas ${}^1M_{78}W_{22}$ presents a denser microstructure than ${}^{0.6}M_{70}W_{30}$ (**Figures 8b' and 8b''**), which is corroborating the role of the metakaolin suggested by the study in compressive strength.

All these observations underline the chemical effect of wollastonite, assuring a better dissolution of the metakaolin, and the steric hindrance effect of glass fibers acting as an anchoring site.

IV- DISCUSSION

In order to understand the influence of the metakaolin and the reinforcement elements on the polycondensation reactions and the properties of geopolymers, the weight loss measured with TGA analysis (42-1000 °C) and the mechanical resistance of geopolymer binders and composites aM_xW_yG_z with $a = 0.6, 0.8$ or 1 (see table 2) has been plotted as function of the

volume of the solution divided by the occupied volume of the metakaolin, the wollastonite and the glass fibers taking into account their water demand (**Figure 9**). The more this ratio is low, the more the species in solution are concentrated. The more the species in solution are concentrated (low ratio), the more the weight loss is low (**Figure 9-a**) and the mechanical strength is high (**Figure 9-b**). As seen previously, the weight loss is linked with the presence of water in the geopolymer network and therefore the polycondensation reaction. The more the available volume is low, the more the weight loss is low. The polycondensation reactions are therefore promoted associated with a high mechanical strength. However, the mechanical properties depend also on the granular skeleton and on the steric hindrance of the glass fibers. This is manifested by a scattering of the points around a general trend. The maximum stress values for a ratio between 0.60 and 0.85 can be explained by the high content of aluminum which governs the mechanical properties as seen in many studies [9, 10, 12]. Thus, the impact of adding reinforcement elements is limited and a maximum value of 55 MPa seems to be reached. The polycondensation reactions as well as the mechanical properties of the material are dependent of the reaction volume. It is therefore possible to control the polycondensation reaction with the metakaolin, wollastonite and glass fibers content which induce the workability and the mechanical properties of the geopolymer composite.

V. CONCLUSION

This study is based on the synthesis of geopolymer composites with different metakaolin, wollastonite and glass fibers contents, and on the investigation of the properties of the fresh and hardened material. FTIR spectroscopy and thermal analyses (DTA and TGA) have been carried out in order to understand the influence of those reinforcement elements on the geopolymerization reactions. Moreover, the viscosity and setting time of the reactive mixtures have been measured to determine their workability, while another part of this study focused on the mechanical strength and the microstructure of the geopolymer composites.

The results highlight that different polycondensation reactions occurred, depending on the nature of the reinforcements used. Adding wollastonite increases the viscosity of the mixture before the setting time on one hand, as well as the mechanical strength of the geopolymer composites by ensuring a better dissolution of the metakaolin on the other hand. Furthermore, the glass fibers lead to a slight enhancement of the viscosity, a ductile failure of the geopolymer composites and act as anchoring sites during the geopolymerization reactions. Finally, the aluminum concentration allows controlling the initial viscosity of the reactive mixture and its setting time, increasing them from 0.18 to 23.82 Pa.s and from 273 to 560 minutes, respectively. This aluminum content has also a significant impact on the microstructure and the compressive strength of the geopolymer composites, raising the later from 22 to 55 MPa.

Thus, for specific applications, the formulation of the geopolymer composites can be monitored and tailored by choosing not only the initial aluminum concentration, but also the nature and amount of reinforcement elements.

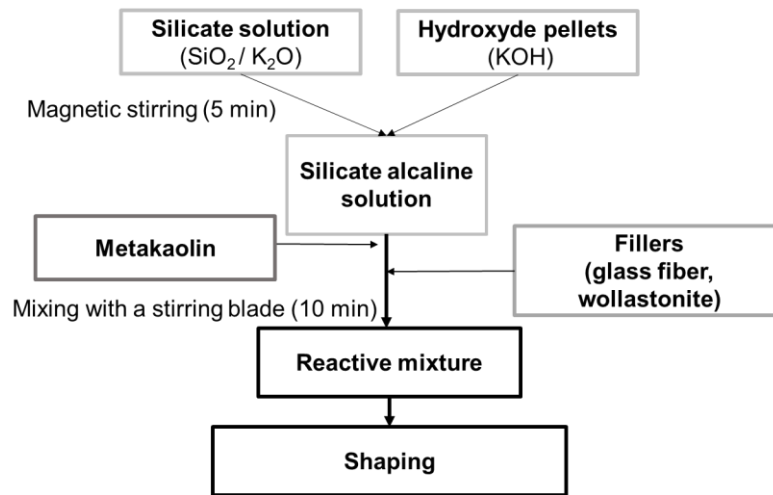


Figure 1. Protocol used to synthesize geopolymer composites.

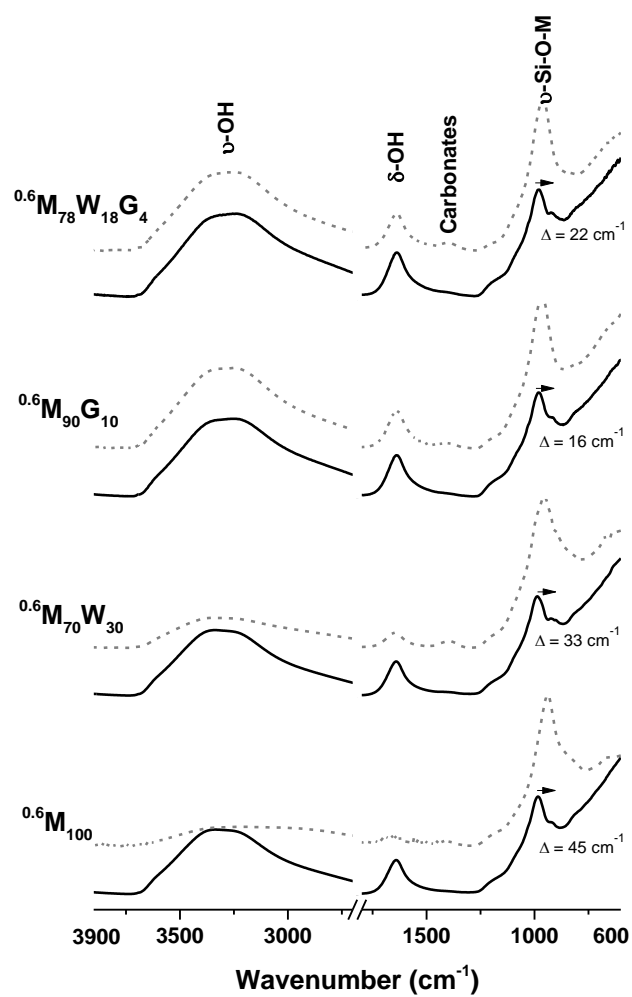


Figure 2. FTIR spectra obtained at — $t = 0$ and at 700 min for the $^{0.6}\text{M}_{100}$, $^{0.6}\text{M}_{70}\text{W}_{30}$, $^{0.6}\text{M}_{90}\text{G}_{10}$ and $^{0.6}\text{M}_{78}\text{W}_{18}\text{G}_4$ samples.

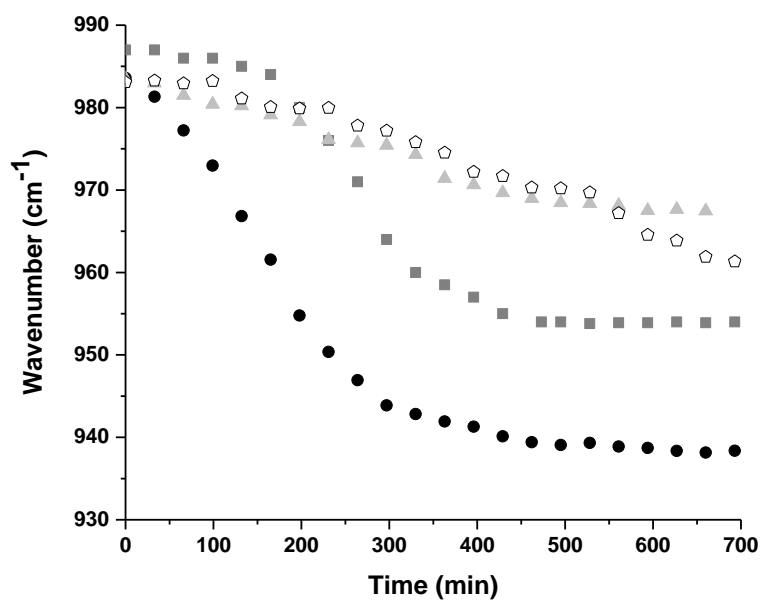


Figure 3. Si-O-M band wavenumber ($\pm 4 \text{ cm}^{-1}$) as a function of time for \bullet $^{0.6}\text{M}_{100}$, \blacksquare $^{0.6}\text{M}_{70}\text{W}_{30}$, \blacktriangle $^{0.6}\text{M}_{90}\text{G}_{10}$ and pentagon $^{0.6}\text{M}_{78}\text{W}_{18}\text{G}_4$ samples.

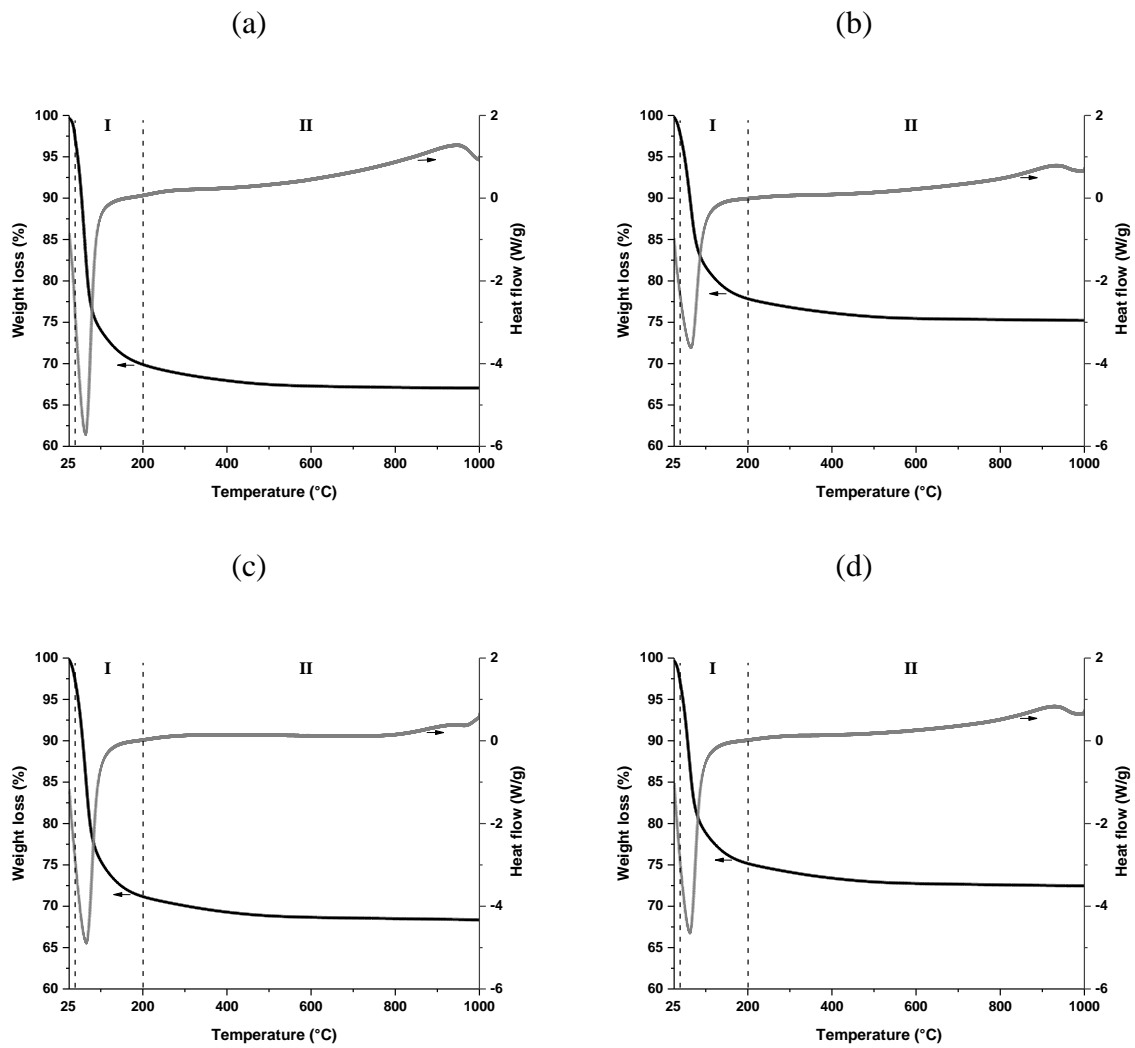


Figure 4. Thermal analysis curves (DTA-TGA) as functions of the temperature for the (a) $^{0.6}\text{M}_{100}$, (b) $^{0.6}\text{M}_{70}\text{W}_{30}$, (c) $^{0.6}\text{M}_{90}\text{G}_{10}$ and (d) $^{0.6}\text{M}_{78}\text{W}_{18}\text{G}_4$ samples.

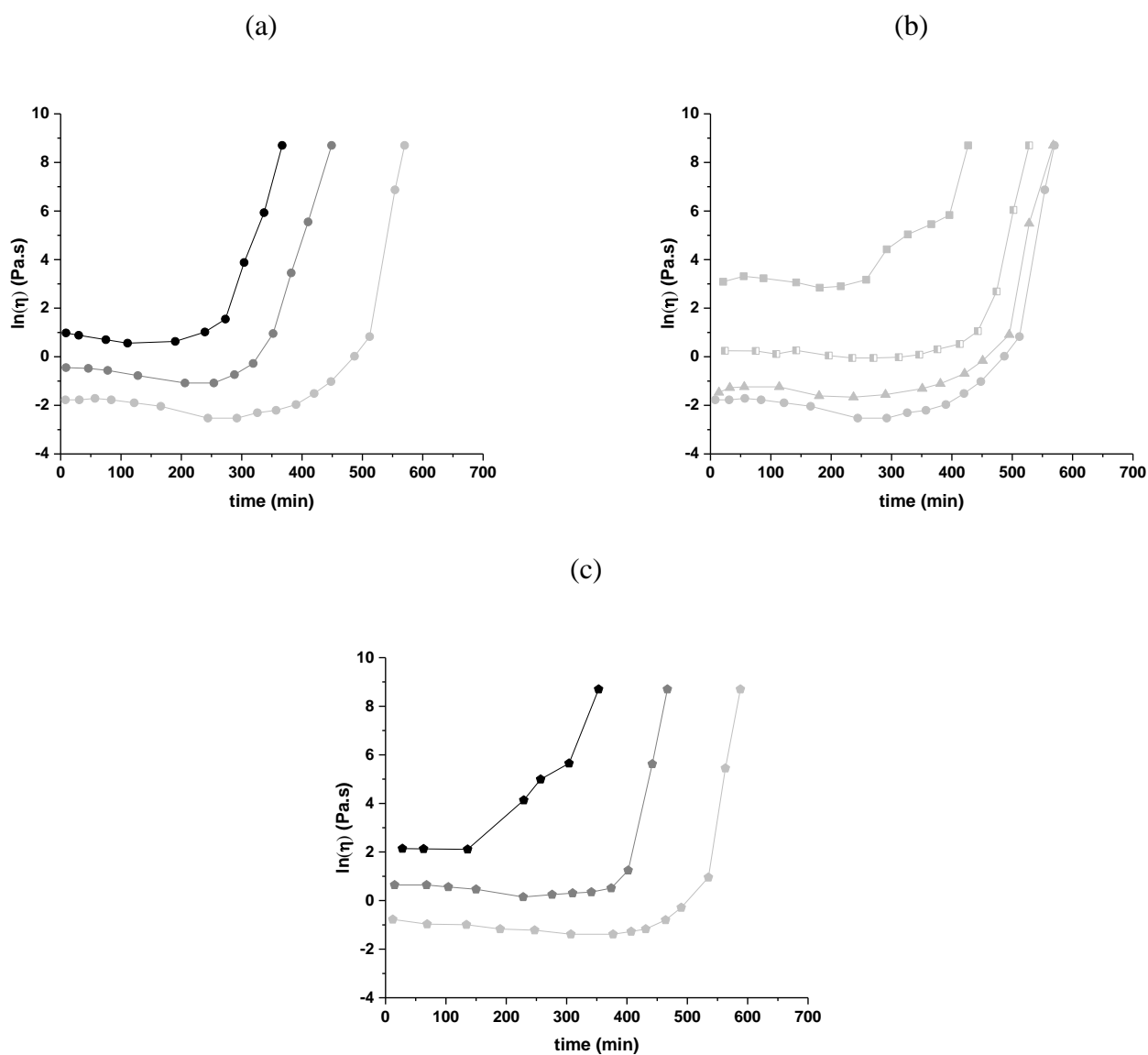


Figure 5. Viscosity η ($\pm 1\%$) as a function of time (± 30 min) for aM_xW_yG_z samples: (a) ${}^aM_{100}$ (a = (\circ) 0.6, (\bullet) 0.8 and (\bullet) 1), (b) (\square) ${}^{0.6}M_{70}W_{30}$, (\blacksquare) ${}^{0.6}M_{45}W_{55}$, (\blacktriangle) ${}^{0.6}M_{90}G_{10}$ and (c) (\circ) ${}^{0.6}M_{78}W_{18}G_4$, (\bullet) ${}^{0.8}M_{85}W_{11}G_4$ (\bullet) ${}^1M_{87}W_{10}G_3$.

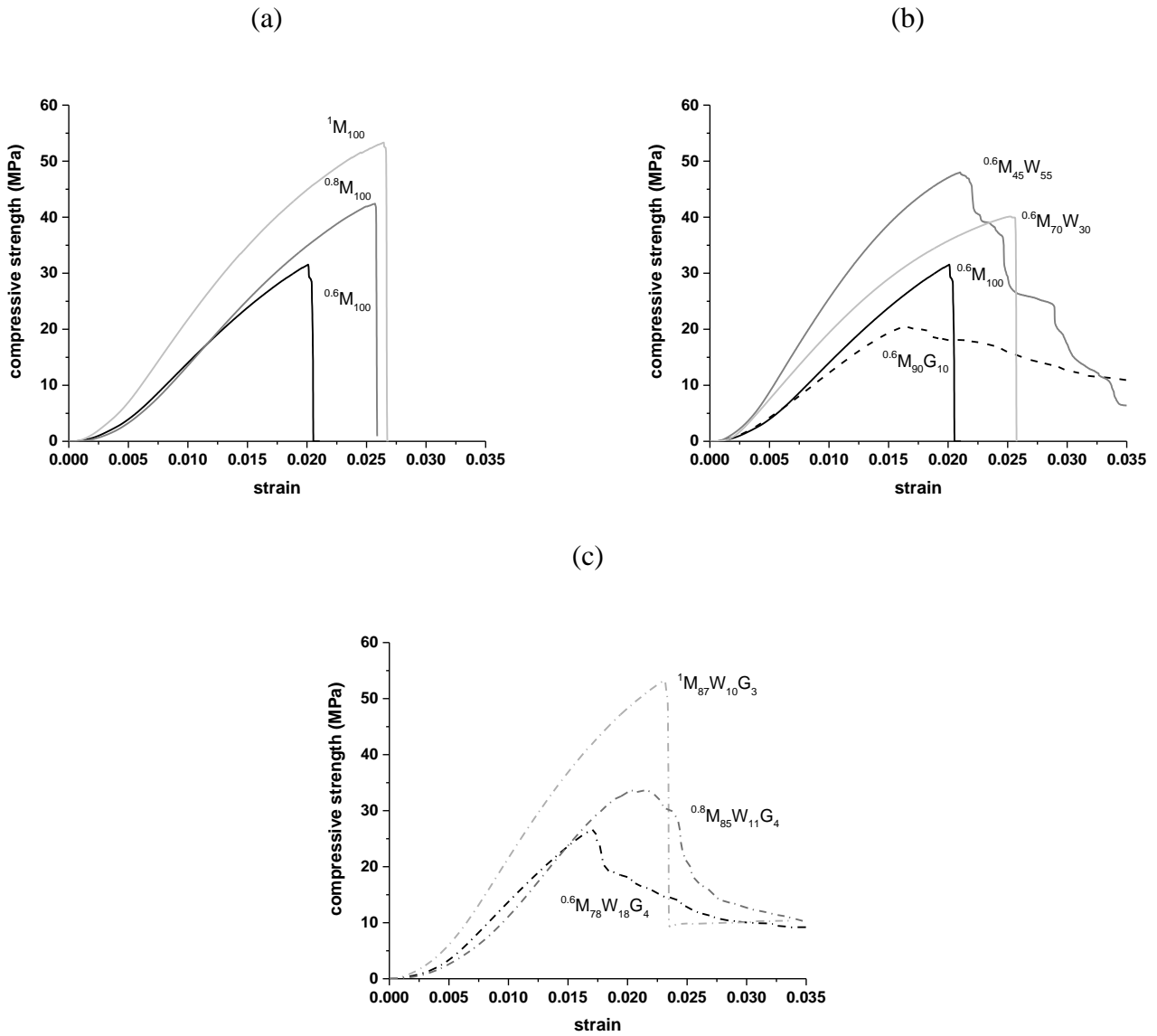


Figure 6. Compressive strength value as a function of the strain for the geopolymer (a) $^aM_{100}$ binders and (b) $^{0.6}M_xW_y$, $^{0.6}M_xG_z$ and (c) aM_xW_yG_z , geopolymer composites.

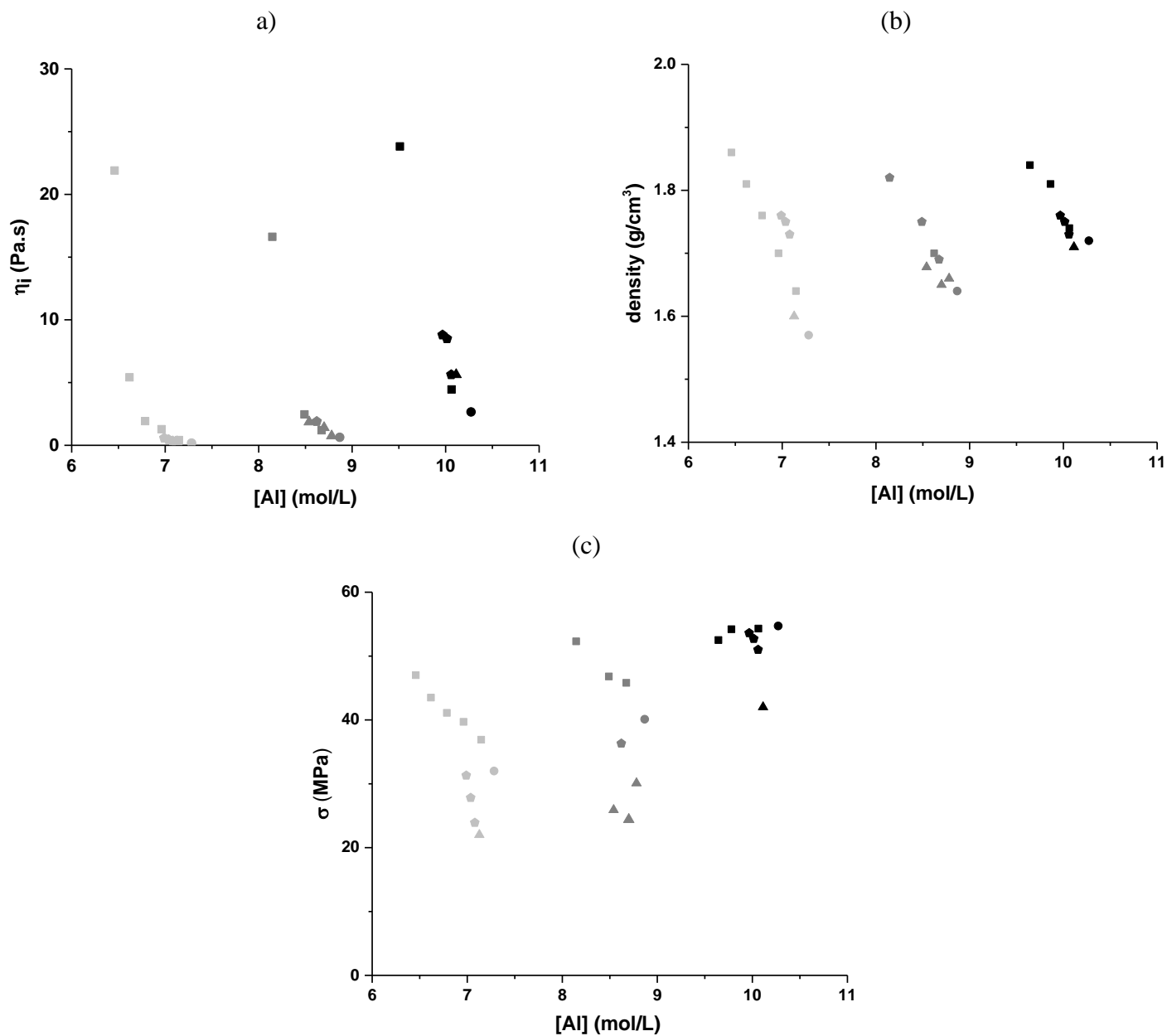


Figure 7. Evolution of (a) the initial viscosity η_i ($\pm 1\%$), (b) the density ($\pm 1 \text{ g/cm}^3$) and (c) the compressive strength σ ($\pm 3 \text{ MPa}$) as functions of the aluminum concentration [Al] for the (●) aM_x , (■) aM_xW_y , (▲) aM_xG_z and (◆) aM_xW_yG_z geopolymer composites, with $a = \text{● } 0.6, \text{● } 0.8$ and $\text{● } 1$ (see Table 2).

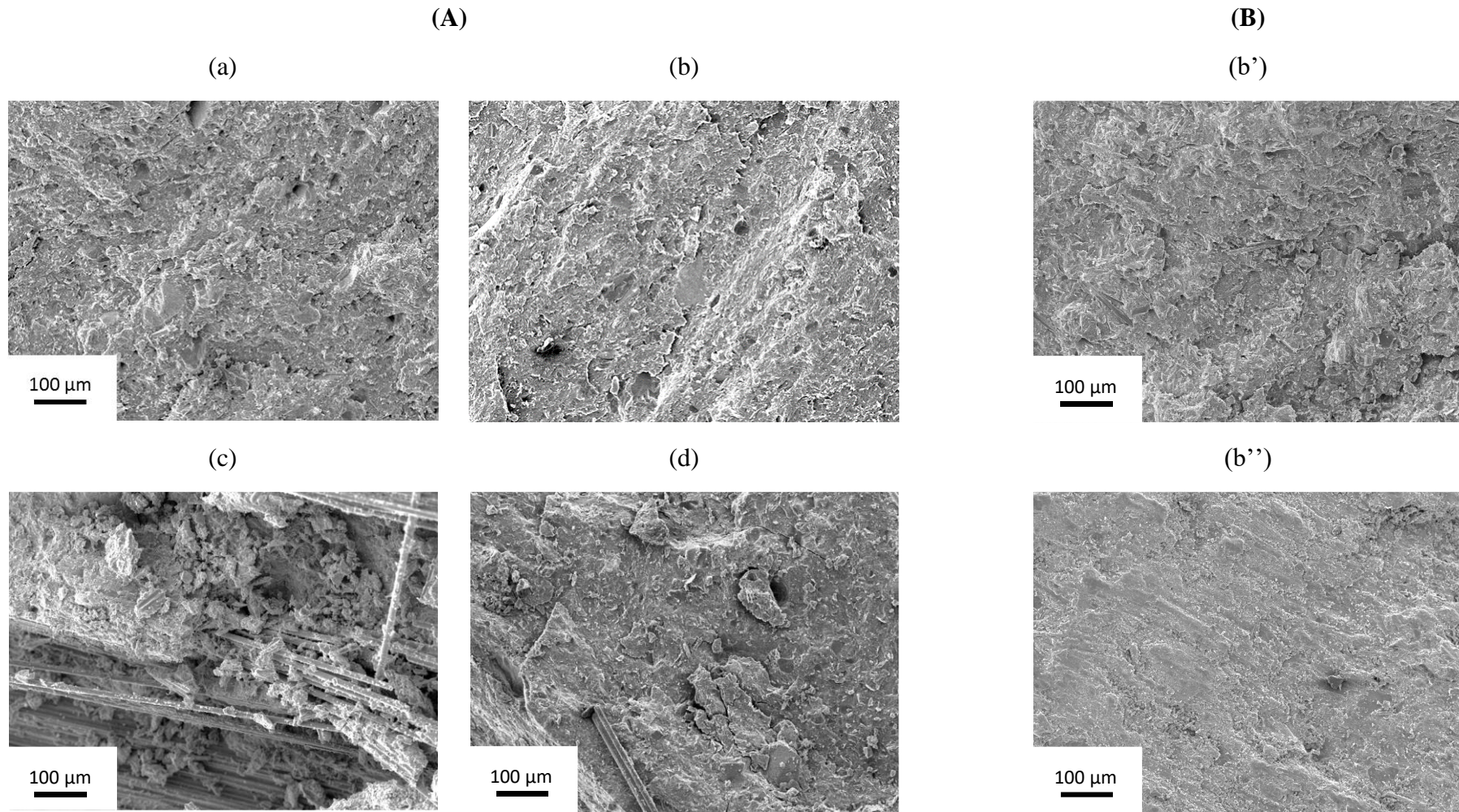


Figure 8. SEM micrographs of the (A) (a) $^{0.8}\text{M}_{100}$, (b) $^{0.8}\text{M}_{74}\text{W}_{26}$, (c) $^{0.8}\text{M}_{92}\text{G}_8$, (d) $^{0.8}\text{M}_{85}\text{W}_{11}\text{G}_4$, and (B) (b') $^{0.6}\text{M}_{70}\text{W}_{30}$ and (b'') $^1\text{M}_{78}\text{W}_{22}$ various formulations.

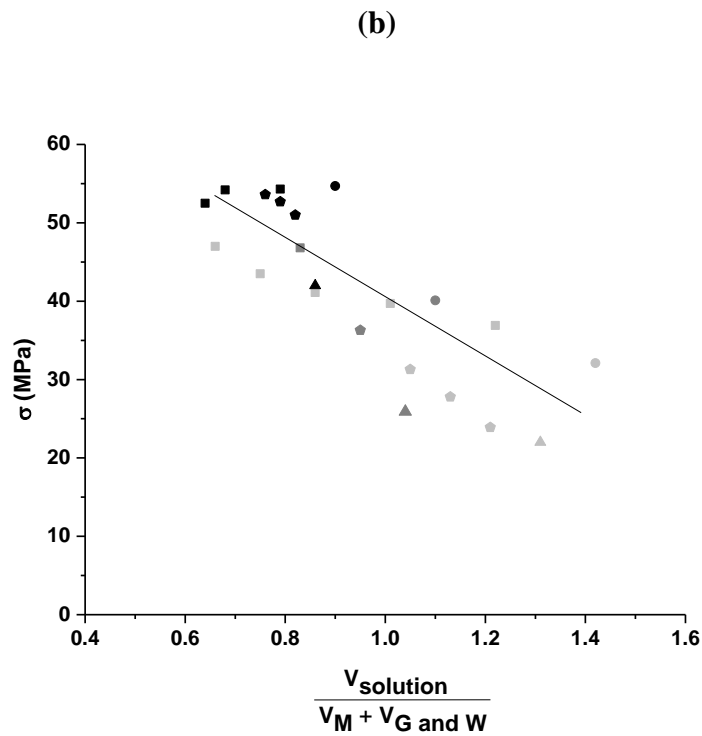
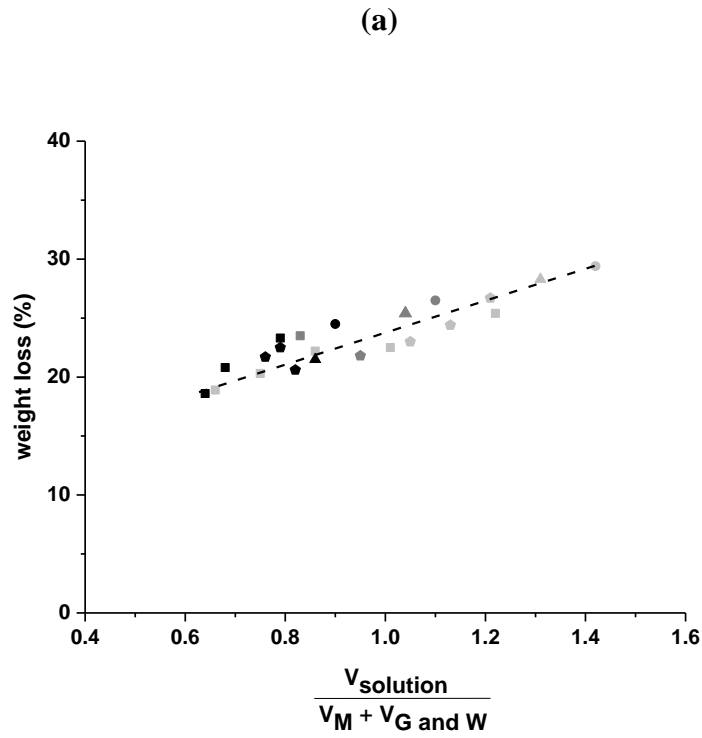


Figure 9. Evolution of (a) the weight loss ($\pm 2\%$) and (b) the compressive strength (± 3 MPa) as function of the ratio $\frac{V_{\text{solution}}}{V_M + V_G \text{ and } W}$ for the (\bullet) aM_x , (\blacksquare) aM_xW_y , (\blacktriangle) aM_xG_z and (\blacklozenge) aM_xW_yG_z geopolymer composites, with $a = \bullet$ 0.6, \bullet 0.8 and \bullet 1 (see Table 2).

Table 1. Name supplier and composition of alkaline solution, metakaolin and reinforcement elements.

	Name	Supplier	Composition (%wt)
Potassium Silicate	S	Woellner	H ₂ O: 76 SiO ₂ : 16 K ₂ O: 8
Potassium hydroxide	KOH	Sigma-Aldrich	KOH : 85 H ₂ O : 15
Metakaolin M1000	M	Imerys	SiO ₂ : 55 Al ₂ O ₃ : 40
AR glass fiber	G	Owens Corning	SiO ₂ : 57 Na ₂ O: 13 ZrO ₂ : 23
Wollastonite	W	Imerys	SiO ₂ : 55 CaO: 45

Table 2. Nomenclature and codes of samples ${}^a\text{M}_x\text{W}_y\text{G}_z$ where a ($= 0.6, 0.8$ or 1) represents the metakaolin to alkaline solution *ratio* in the binder and x, y and z the weight percentage of metakaolin (M), wollastonite (W) and glass fibers (G), respectively.

Nomenclature	x (%wt)	y (%wt)	z (%wt)	Code
${}^{0.6}\text{M}_x$	100	0	0	●
${}^{0.6}\text{M}_x\text{W}_y$	85 – 45	15 – 55	0	■
${}^{0.6}\text{M}_x\text{G}_z$	90	0	10	▲
${}^{0.6}\text{M}_x\text{W}_y\text{G}_z$	83 – 73	10 - 25	7 - 2	◆
${}^{0.8}\text{M}_x$	100	0	0	●
${}^{0.8}\text{M}_x\text{W}_y$	74	26	0	■
${}^{0.8}\text{M}_x\text{G}_z$	92	0	8	▲
${}^{0.8}\text{M}_x\text{W}_y\text{G}_z$	85	11	4	◆
${}^1\text{M}_x$	100	0	0	●
${}^1\text{M}_x\text{W}_y$	93 – 70	7 – 30	0	■
${}^1\text{M}_x\text{G}_z$	94	0	6	▲
${}^1\text{M}_x\text{W}_y\text{G}_z$	91 - 84	5 - 15	4 - 1	◆

VI. REFERENCES

- [1] C. Dupuy, A. Gharzouni, N. Texier-Mandoki, X. Bourbon, S. Rossignol, “Alkali-activated materials based on Callovo-Oxfordian argillite: formation structure and mechanical properties”, *J. Ceram. Sci. Technol.*, vol. 09, pp. 127-140, 2018.
- [2] J. Davidovits, *Geopolymer Chemistry and Applications*, 2nd ed. Saint-Quentin, France: Institut Geopolymer, 2008.
- [3] J.L. Provis, “Geopolymers. Structure, Processing”, *Properties and Industrial Applications*, Woodhead Publishing Limited, 2009.
- [4] E. Prud’homme, P. Michaud, E. Joussein, J.-M. Clacens, S. Rossignol, “Role of alkaline cations and water content on geomaterial foams: Monitoring during formation”, *Journal of Non-Crystalline Solids*, vol. 357, pp. 1270–1278, 2011.
- [5] A. Gharzouni, E. Joussein, B. Samet, S. Baklouti, S. Rossignol, “Effect of the reactivity of alkaline solution and metakaolin on geopolymer formation”, *Journal of Non-crystalline Solids*, vol. 410, pp. 127-134, 2015.
- [6] M. Romagnoli, P. Sassatelli, M. Lassinanti, Gualtieri, G. Tari, “Rheological characterization of fly-ash-based suspensions”, *Construction and Building Materials*, vol. 65, pp. 526-534, 2014.
- [7] M. Arnoult, M. Perronnet, A. Autef, S. Rossignol, “Geopolymer synthesized using reactive or unreactive aluminosilicate. Understanding of reactive mixture”, *Materials Chemistry and Physics*, vol. 237, article 121837, 2019.
- [8] M. Arnoult, M. Perronnet, A. Autef, S. Rossignol, “How to control the geopolymer setting time with the alkaline silicate solution”, *Journal of non-Crystalline Solids*, vol. 495, pp. 59-66, 2018.
- [9] L. Vidal, A. Gharzouni, S. Rossignol, “Alkaline silicate solutions: an overview of their structure, reactivity and applications”, *2nd edition of the Handbook of Sol’Gel Science and Technology*, pp. 181-204, 2016.
- [10] A. Autef, E. Joussein, G. Gasgnier, S. Pronier, I. Sobrados, J. Sanz, S. Rossignol, “Role of metakaolin dehydroxylation in geopolymer synthesis”, *Powder Technology*, vol. 250, pp. 33-39, 2013.
- [11] A. Gharzouni, I. Sobrados, E. Joussein, S. Baklouti, S. Rossignol, “Control of polycondensation reaction generated from different metakaolins and alkaline solutions”, *J. Ceram. Sci. Technol.*, vol. 08, pp. 365-376, 2017.
- [12] N.A. Jaya, Y.M. Liew, C.Y. Heah, M.M.A.B Abdullah, “Effect of solid to liquid ratios on metakaolin geopolymers”, *AIP Conference Proceedings 2045*, 020099, 2018.
- [13] H. Cheng, K. Lin, R. Cui, C. Hwang, T. Cheng, Y. Chang, “Effect of solid to liquid ratios on the properties of waste catalyst-metakaolin based geopolymer”, *Construction and Building Materials*, vol. 88, pp. 74-83, 2015.
- [14] E. Prud’homme, E. Joussein, C. Peyratout, A. Smith, S. Rossignol, “Consolidated geomaterials from sand or industrial waste”, *Ceram. Eng. Sci.*, vol. 30, pp. 314–324, 2010.
- [15] B. Panda, C. Unluer, M. J. Tan, “Extrusion and rheology characterization of geopolymer nanocomposites used in 3D printing”, *Composites part B*, vol. 176, 2019.
- [16] C. Kuenzel, L. Li, L. Vandeperre, A.R. Boccaccini, C.R. Cheeseman, “Influence of sand on the mechanical properties of metakaolin geopolymers”, *Construction and Building Materials*, vol. 66, pp. 442-446, 2014.
- [17] C. Dupuy, J. Havette, A. Gharzouni, N. Texier-Mandoki, X. Bourbon, S. Rossignol, “Metakaolin-based geopolymer: formation of new phases influencing the setting with the use of additives”, *Construction and Building Materials*, vol. 200, pp. 272-281, 2019.

-
- [18] R.A. Sé Ribeiro, M.G. Sà Ribeiro, W.M. Kriven, "A review of particle and fiber reinforced metakaolin based geopolymer composites", *J. Ceram. Sci. Technol.*, vol. 8, pp. 302-322, 2017.
- [19] N. Ranjbar, M. Zhang, "Fiber-reinforced geopolymer composites: a review", *Cement and concrete composites*, vol. 107, 103498, 2020.
- [20] J. Davidovits, "Geopolymer: inorganic polymeric new materials", *Journal of thermal analysis*, vol. 37, pp. 1633-1656, 1991.
- [21] Q. Zhao, B. Nair, T. Rahimian, P. Balaguru, P. Novel, "geopolymer based composites with enhanced ductility", *Journal of Materials Science*, vol. 42, pp. 3131-3137, 2007.
- [22] Z. Li, Y. Zhang, X. Zhou, "Short fiber reinforced geopolymer composites manufactured by extrusion", *Journal of Materials in Civil Engineering*, vol. 17, pp. 624-631, 2005.
- [23] A.C.P Santos, J. Ortiz-Lozano, N. Villegas, A. Aguado, "Experimental study about the effects of granular skeleton distribution on the mechanical properties of self-compacting concrete (SCC)", *Construction and Building Materials*, vol. 78, pp. 40-49, 2015.
- [24] T. Lin, D. Jia, P. He, M. Wang, D. Liang, "Effects of fiber length on mechanical properties and fracture behaviour of short carbon fiber reinforced geopolymer matrix composites", *Materials Science and Engineering*, vol. 497, pp. 181-185, 2008.
- [25] J. Yuan, P. He, D. Jia, X. Lanlan, S. Yan, D. Cai, Z. Yang, X. Duan, S. Wang, Y. Zhou, "SiC fiber reinforced geopolymer composites, part 1: short SiC fiber", *Ceramics International*, vol. 42, pp. 5345-5352, 2015.
- [26] M. Welter, M. Schmücker, K.J.D. MacKenzie, "Evolution of the fibre-matrix interactions in basalt-fibre-reinforced geopolymer matrix composites after heating", *J. Ceram. Sci. Tech.*, vol. 06, pp. 17-24, 2015.
- [27] E. Rill, D. Lowry, W.M. Kriven, "Properties of basalt fiber reinforced geopolymer composites", *Strategic Materials and Computational Design*, vol. 31, pp. 57-67, 2010.
- [28] M. Steinerova, L. Matulova, P. Vermach, J. Kotas, "The Brittleness and chemical stability of optimized geopolymer composites", *Materials*, vol. 10, pp. 396-416, 2017.
- [29] R. Novais, J. Carvalheiras, M.P. Seabra, R.C. Pullar, J.A. Labrincha, "Effective mechanical reinforcement of inorganic polymers using glass fibre waste", *Journal of Cleaner Production*, vol. 166, pp. 343-349, 2017.
- [30] T. Alomayri, "Effect of glass microfibre addition on the mechanical performances of fly ash-based geopolymer composites", *Journal of Asian Ceramic Societies*, vol. 5, pp. 334-340, 2017.
- [31] B. Nematollahi, J. Sanjayan, J.X.H. Chai, T.S. Lu, "Properties of Fresh and Hardened Glass Fiber Reinforced Fly Ash Based Geopolymer Concrete", *Key Engineering Materials*, vols. 594-595, pp. 629-633, 2014.
- [32] N.M.P Low, J.J. Beaudoin, "Mechanical properties of high performance cement binders reinforced with wollastonite micro-fibres", *Cement and Concrete Research*, vol. 22, pp. 981-989, 1992.
- [33] F. Silva, C. Thaumaturgo, "Fibre reinforcement and fracture response in geopolymeric mortars", *Fatigue fract. Enging. Mater. Struct.*, vol. 26, pp. 167-172, 2003.
- [34] D. Nurjaya, S. Astutiningsih, A. Zulfia, "Thermal effect on flexural strength of geopolymer matrix composite with alumina and wollastonite as fillers", *International journal of technology*, vol. 3, pp. 462-470, 2015.
- [35] L. Martinie, P. Rossi, N. Roussel, "Rheology of fiber reinforced cementitious materials: classification and prediction", *Cement and concrete research*, vol. 40, pp. 226-234, 2010.
- [36] L. Vickers, W.D.A. Rickard, A. van Riessen, "Strategies to control the high temperature shrinkage of fly ash based geopolymer" *Thermochimica Acta*, vol. 580, pp. 20-27, 2014
- [37] A. Gharzouni, I. Sobrados, E. Joussein, S. Baklouti, S. Rossignol, "Predictive tools to control the structure and the properties of metakaolin based geopolymer materials", *Colloids and Surfaces A: Physiochem. Enf. Aspects*, vol. 511, pp. 212-221, 2016.

-
- [38] A. Gharzouni, “Contrôle de l'attaque des sources aluminosilicates par la compréhension des solutions alcalines”, PhD Thesis, Université de Limoges, France, 2016.
- [39] Grünewald S., Performance-based design of self-compacting fibre reinforced concrete, PhD-thesis, Technische Universiteit Delft, Netherlands, 2004.
- [40] M. Rowles, B O'Connor, “Chemical optimization of the compressive strength of aluminosilicate geopolymers by sodium silicate activation of metakolinite”, *J. Mater. Chem.*, vol. 13, pp. 1161-1165, 2003.
- [41] A. Gharzouni, B. Samet, S. Baklouti, E. Joussein, S. Rossignol, “Addition of low reactive clay into metakaolin-based geopolymer formulation : Synthesis, existence domains and properties”, *Powder technology*, vol. 288, pp. 212-220, 2016.